JOURNAL OF MATERIALS SCIENCE 33 (1998) 723–728

Preparation of nanocrystalline YSZ powders by the plasma technique

J. GRABIS, A. KUZJUKEVICS, D. RASMANE
Institute of Inorganic Chemistry, Latvian Academy of Sciences, Salaspils, LV-2169, Latvia
M. MOGENSEN, S. LINDEROTH
Materials Department, Risø National Laboratory, DK-4000 Roskilde, Denmark

A plasma synthesis method has been devised to produce nanosize YSZ powders with various yttria contents. The powders are synthesized by introducing a mixture of coarse-grained zirconia and yttria into an r.f. inductively coupled plasma flame. The average particle size of the as-prepared powders is in the range 20–40 nm and the specific surface area is 18–50 $m^2 g^{-1}$. The phase and granulometric composition of the produced powders depend on the degree of evaporation of raw powders, reagent concentration in the gas flow and quenching rate, and on the content of Y_2O_3. Up to 5.5 mol % yttria, the major phase of nanosize powders is tetragonal ZrO_2, mostly as the non-transformable (t′) form. For yttria contents higher than 6 mol %, the major phase is cubic ZrO_2. © *1998 Chapman & Hall*

1. Introduction

Yttria-stabilized zirconia (YSZ) has many applications because of its high melting point, good corrosion resistance, high fracture toughness, low thermal and high ionic conductivity. Physical characteristics of sintered ceramics strongly depend on the morphology of the starting powders and on the method used for their syntheses. In order to produce fully dense ceramics of uniform microstructure and consistent properties, the use of a homogeneous active nanosize precursor powder is essential, for both mechanical and electrical application.

Owing to the increased importance of nanosize powders, many non-conventional powder preparation techniques have been developed such as sol–gel [1], spray pyrolysis [2], laser-sputtering [3], gas-phase condensation [4] and plasma synthesis [5, 6]. Plasma synthesis of zirconia powder provides an attractive alternative to conventional methods because ceramic made of plasma-produced YSZ powders shows increased resistance to low-temperature ageing [5, 6]. However, the developed plasma technique allows YSZ powder to be produced with a particle size of 35–200 μm [6] or nanosized zirconia powder, which afterwards must be coated with yttria by a pigment-coating technology [5].

The aim of the present study was to develop a plasma technique for the direct preparation of nanosize YSZ powders by evaporation of pre-mixed oxides in the plasma flame.

2. Experimental procedure

A schematic diagram of the apparatus used for the present study is shown in Fig. 1. The apparatus consists of an r.f. oscillator (maximum power 100 kW, frequency 5.28 MHz), a quartz tube (65 mm diameter) with a three-turn induction coil, a water-cooled stainless steel reaction chamber with following heat exchangers and cloth filter for powder collecting, as well as raw powder and gas supply systems. The inductively coupled plasma (ICP) torch operates with air as the plasma-forming gas at flow rates of 7.6–8.5 $m^3 h^{-1}$. The raw powder, a mixture of the required amounts of commercially available zirconia (99.8%) and yttria (99.9%) was injected into the tail of the plasma flame by transporting gas through four tubes (3 mm diameter) welded in a water-cooled flange (40, 50 or 70 mm diameter), or with four water-cooled probes at a distance of 15 mm from the plasma flame axis.

The optimal conditions for complete evaporation of raw powders were determined by investigating the influence of precursor grain size, the injection mode and feeding rate on the particle size, particle-size distribution and specific surface area of the prepared powders. YSZ particle condensation and subsequent growth processes were controlled by quenching by air (3.4–6.0 $m^3 h^{-1}$) introduced into the reaction chamber.

The plasma synthesis products were characterized by conventional chemical analysis and X-ray diffraction using filtered CuK_α radiation. The phase composition was calculated from the ratio of integrated intensities of diffraction maxima [7, 8]. The specific surface area (SSA) of as-prepared powders was determined by the BET argon adsorption–desorption method. The average particle size was calculated from the value of SSA assuming spherical particle shape and controlled by transmission electron microscopy (TEM) and scanning electron microscopy (SEM). The presence of coarse particles with size above 1 μm in

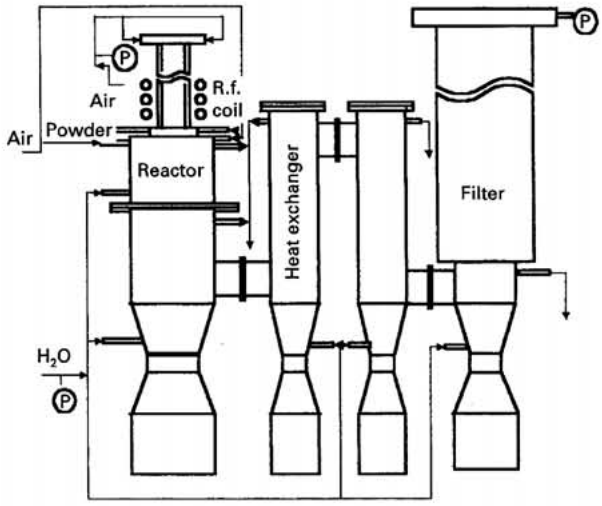

Figure 1 Schematic view of the plasma apparatus.

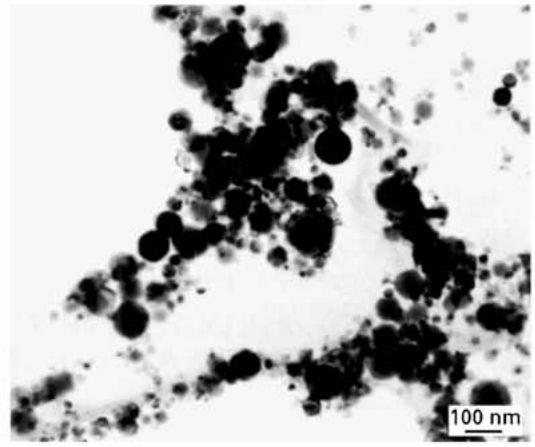

Figure 2 Transmission electron micrograph of the fine particle fraction of YSZ powder.

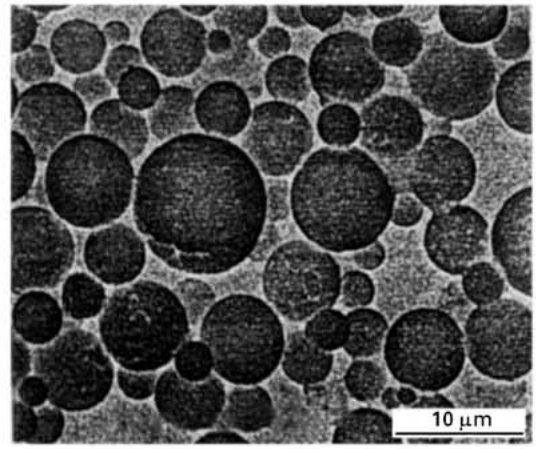

Figure 3 Scanning electron micrograph of the coarse particle fraction of YSZ powders.

prepared powder was detected by sedimentation as follows. A weighed amount of an as-prepared powder (0.3 g) was dispersed in pure ethanol (300 ml) by ultrasonic agitation (44 kHz) for 20 min. Afterwards, the suspension was allowed to sediment for 20 min. The suspension of the fine particle fraction in ethanol was separated from the sediment, and after evaporation of ethanol, the fine and coarse particle fractions were collected and examined.

Selected as-prepared powders were annealed in the temperature range between 500 and 1250 °C for 2 h followed by furnace cooling to study the effect of heat treatment on phase composition. To study a possible stress-induced tetragonal-to-monoclinic transformation, some powders were pressed into pellets and further characterized by X-ray diffraction (XRD).

3. Results and discussion

3.1. Particle-size distribution in as-prepared powders

The raw powder injection mode, feeding rate and grain size are essential parameters of plasma synthesis, determining the particle size, size distribution and phase composition of the as-prepared powders. A careful optimization of the injection parameters was found to be necessary in order to avoid a very broad or even bimodal particle-size distribution of the synthesized powders. For example, particles with a size in the 0.005–15 μm range were found in some samples of produced powders. From this, the fine (<1 μm) and coarse ($\geqslant 1$–15 μm) particle fractions can be separated by sedimentation. Figs 2 and 3 are illustrative transmission and scanning electron micrographs of the fine and coarse particles, respectively. As revealed by XRD patterns, the fine fraction of YSZ powders consists of a mixture tetragonal and cubic zirconia phases. The coarse particle fraction, besides these, usually contains monoclinic zirconia and free yttria.

Table I shows the content of coarse fraction, chemical and phase composition of the as-prepared powders, depending on the raw powder grain size. Powders were synthesized with a raw powder feeding rate of 0.9 $kg\,h^{-1}$ and inlet flange with a diameter of 70 mm. It is seen that the raw powder with narrow size distribution decreases the content of coarse fraction and the difference in Y_2O_3 content of both fractions. The same is observed if the grain size of raw ZrO_2 powder is decreased from 40–60 μm to 10–40 μm (series 2 and 3). However, a further decrease in the raw powder grain size to 0.5–10 μm gives the opposite result – the content of coarse fraction increases (series 4).

Using 10–40 μm ZrO_2 and Y_2O_3 powders, the injection mode was then varied while keeping the feeding rate constant at 0.9 $kg\,h^{-1}$. From Table II it can be clearly seen how the content of coarse fraction changes with decreasing diameter of the inlet flange (series 5–7). In series 8, water-cooled probes were used, inserted at a distance of 15 mm from the plasma flame axis. This modification resulted in a very small content of coarse fraction. Moreover, no difference in chemical and phase composition is observed between coarse and fine particle fractions.

The presence of the coarse particles can be explained by incomplete evaporation of the raw powder and coagulation of non-evaporated droplets in the plasma flame. The plasma flame is characterized by a certain temperature distribution in radial and

TABLE I Dependence of the characteristics of YSZ powders on particle sizes of raw materials injected into the plasma through four tubes welded in a water-cooled flange (70 mm diameter) at the powder feeding rate of 0.9 kg h^{-1}

No.	Particle sizes of raw powders (μm)	As-prepared YSZ powders			Fraction of the coarse particles (1–15 μm)			Fraction of the fine particles (≤1 μm)	
		S (m^2 g^{-1})	Y_2O_3 (mol %)	Phases	Amount (wt %)	Y_2O_3 (mol %)	Phases	Y_2O_3 (mol %)	Phases
1	ZrO_2 0.5–40 Y_2O_3 0.5–40	24.2	6.0	m-, t-, c-ZrO_2 Y_2O_3	13.6	6.9	m-, t-, c-ZrO_2 Y_2O_3	5.3	t-, c-ZrO_2
2	ZrO_2 10–40 Y_2O_3 10–40	26.8	6.0	t-, c-ZrO_2	4.6	6.2	t-, c-ZrO_2,m-ZrO_2 (tr.)	5.8	t-, c-ZrO_2
3	ZrO_2 40–60 Y_2O_3 10–40	22.5	6.0	m-, t-, c-ZrO_2	7.1	6.5	m-, t-, c-ZrO_2	5.7	t-, c-ZrO_2
4	ZrO_2 0.5–10 Y_2O_3 0.5–10	23.6	6.0	m-, t-, c-ZrO_2 Y_2O_3	10.4	6.6	m-, t-, c-ZrO_2 Y_2O_3	5.5	t-, c-ZrO_2

TABLE II Dependence of the characteristics of the YSZ powders on injection mode of the raw powder at the feeding rate of 0.9 kg h^{-1}, particle sizes of ZrO_2 10–40 μm, Y_2O_3 10–40 μm

No.	Mode of raw particle injection	As-prepared YSZ powders			Fraction of the coarse particles			Fraction of the fine particles	
		S (m^2 g^{-1})	Y_2O_3 (mol %)	Phases	Amount (wt %)	Y_2O_3 (mol %)	Phases	Y_2O_3 (mol %)	Phases
5	Through four tubes welded in a water cooled flange (70 mm diameter)	26.8	6.0	t-, c-ZrO_2	4.6	6.2	t-, c-ZrO_2 m-ZrO_2 (tr.)	5.9	t-, c-ZrO_2
6	Through four tubes welded in a water cooled flange (50 mm diameter)	29.2	6.0	t-, c-ZrO_2	3.5	6.1	t-, c-ZrO_2	5.9	t-, c-ZrO_2
7	Through four tubes welded in a water cooled flange (40 mm diameter)	33.0	6.0	t-, c-ZrO_2	1.8	6.0	t-, c-ZrO_2	6.0	t-, c-ZrO_2
8	By water-cooled probes at a distance 15 mm from the axis of the plasma	28.9	6.0	t-, c-ZrO_2	~0.5	6.0	t-, c-ZrO_2	6.0	t-, c-ZrO_2

longitudinal directions. To reach the complete evaporation of the raw powders, all grains should be introduced into the central region of the plasma flame with the gas temperature of 5400–5800 K. The grain size should also be sufficiently small, because the duration time of grains in the high-temperature region of the flame is very short (~5 ms). On the other hand, the penetration depth of raw grains into the plasma flame depends on their mass and velocity. The motion trajectories of small grains (0.5–10 μm) even at a high injection velocity, cross mainly the outer layer of the flame where the gas temperature is too low for complete evaporation. These grains can only reach the melting temperature and, hence, form the coarse particles in the synthesis product. From Table I, it follows that zirconia and yttria grain sizes of 10–40 μm are large enough to penetrate into the inner part of plasma flame and, at the same time, small enough to reach the highest degree of evaporation for a given injection conditions. In this case, the presence of the coarse particles in as-prepared powders can be caused by the velocity distribution of grains which determines a different penetration depth of raw grains into the flame. Decreasing the diameter of the raw powder injection flange, or injection through water-cooled probes immersed into the plasma flame, reduce the content of the coarse particle fraction and improve the phase composition of the produced YSZ powders (Table II). This is because the probability increases for grains to reach the inner region of the plasma flame.

From the results given above, it follows that the injection of raw powders with a grain size of 10–40 μm through water-cooled probes or a flange with a diameter of 40 mm, creates the best conditions for evaporation of the raw oxides and producing YSZ powders with more uniform granulometric, phase and chemical composition. These conditions were used to study the effect of the raw powder feeding rate on the content of coarse fraction and specific surface area of as-prepared powders. As shown in Fig. 4, a further decrease of the content of coarse fraction is possible by reducing the raw powder feeding rate below 0.6–0.7 kg h^{-1} or increasing the flow rate of the quenching gas (and consequently increasing the quenching rate of the produced particles). Lower raw powder feeding rate and higher

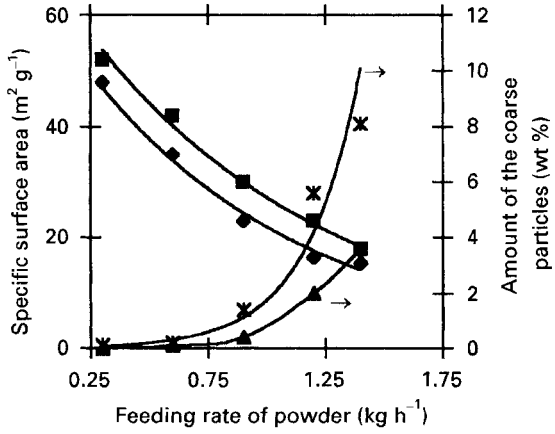

Figure 4 (■, ◆) Specific surface area and (×, ▲) amount of coarse particles of YSZ as function of feeding rate of powder at a flow rate of cooling gas of (◆, ×) 3.4 and (■, ▲) 6.0 $m^3 h^{-1}$, and an inlet diameter of 40 mm.

quenching rate reduce the duration time of primary particles in the growing zone and the growth of the secondary particles formed by a coalescence of the liquid droplets.

In such a way, optimization of the evaporation and condensation conditions in the ICP flame resulted in improved granulometric and phase composition of produced powders. The following process parameters were used for manufacturing YSZ powders: raw powder grain size, 10–40 μm; feeding rate, 0.4–0.6 kg h^{-1}; quenching gas rate, 4.5–6.0 $m^3 h^{-1}$; raw powder injection mode, flange with a diameter of 40 mm or water-cooled probes.

By maintaining the above-mentioned process parameters, spherical nanosized zirconia and YSZ powders can be produced with an average particle size of 20–40 nm (specific surface area of 18–50 $m^2 g^{-1}$).

3.2. Phase composition of nanocrystalline powders

According to the XRD analysis, non-doped zirconia powder is a mixture of monoclinic and tetragonal phases. The content of the tetragonal phase depends on the average particles size and increases from 65% to 80% if the specific surface area changes from 18 $m^2 g^{-1}$ to 30 $m^2 g^{-1}$ (Table III). This can be explained by the suggestion that a lower surface energy stabilizes the tetragonal form in very small zirconia particles [9].

Fig. 5 shows the phase composition of YSZ powders versus yttria content. The major phase of as-prepared powders is the tetragonal ZrO_2 for yttria content <4.5–5.5 mol %. Traces of the monoclinic phase are also detectable below 4.5 mol % Y_2O_3. The appearance of m-ZrO_2 in plasma-prepared YSZ with the yttria content around 3–4.5 mol % is most likely caused by a certain inhomogeneity of yttria distribution in as-prepared powders. For yttria contents higher than 6 mol %, the major phase is the cubic ZrO_2. However, traces of t-ZrO_2 are visible on the XRD pattern of the sample Z8.1Y with an yttria content of 8.1 mol %, as revealed by the presence of the 1 1 2 maximum around $2\theta = 42.5°$. This also might be a result of inhomogeneous yttria distribution in as-prepared powders.

TABLE III The content of tetragonal phase of zirconia as a function of the specific surface area and average particle size of as-prepared zirconia powder

No.	Specific surface area ($m^2 g^{-1}$)	Average size (nm)	t-ZrO_2 (%)
1	18	57	65
2	24	42	72
3	28	36	77
4	30	33	80

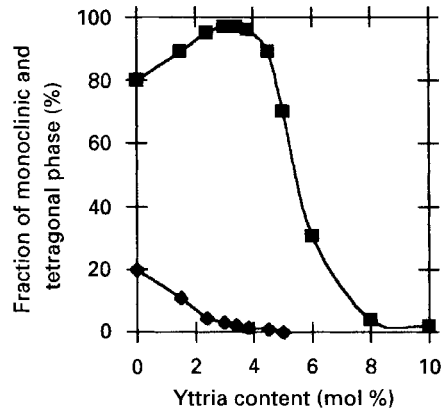

Figure 5 Fraction of (◆) monoclinic and (■) tetragonal phases of zirconia versus yttria content in YSZ powder. Inlet flange diameter 40 mm, flow rate of cooling gas 6.0 $m^3 h^{-1}$ and feeding rate of powder 0.6 kg h^{-1}.

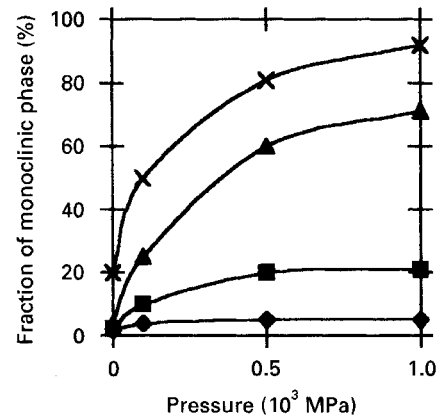

Figure 6 Change of fraction of monoclinic phase of zirconia with dry pressing pressure at Y_2O_3 contents (mol %): (×) 0, (▲) 2.4, (■) 3.4 and (◆) 3.8.

Results of stress-induced transformation during pressing (Fig. 6) and annealing (Fig. 7) of as-prepared powders show the tetragonal phase of non-doped ZrO_2 is metastable. Under pressure or on heating at temperatures higher than 550 °C, it transforms to the monoclinic phase. The tetragonal-to-monoclinic phase transformation at 550 °C agrees with the data for ultrafine ZrO_2 prepared by the spray-ICP technique [10]. This cannot be associated with the particle growth which starts only at temperatures of

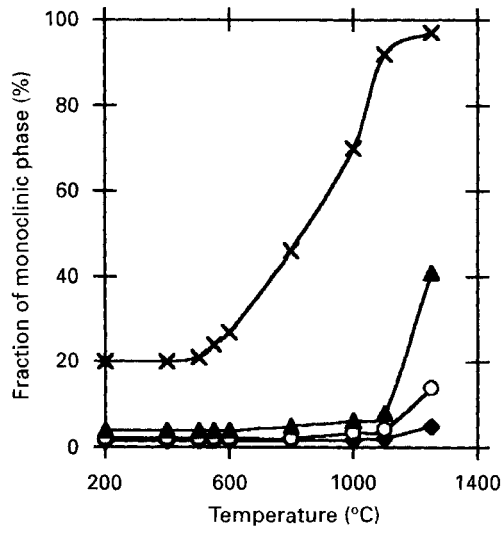

Figure 7 Change of fraction of monoclinic phase of zirconia with calcination temperature at Y_2O_3 contents (mol %): (×) 0, (▲) 2.4, (○) 3.4 and (◆) 3.8.

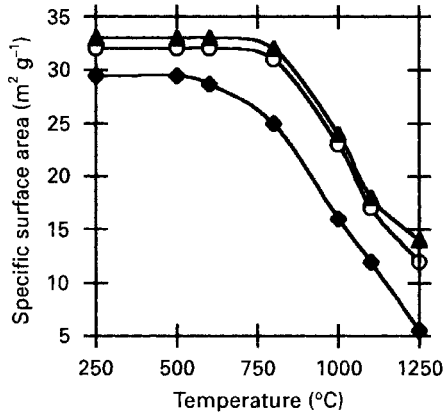

Figure 8 Change of specific surface area of powder with calcination temperature at Y_2O_3 contents (mol %): (▲) 8, (○) 2.4 and (◆) 0.

650–700 °C as revealed by the changes of SSA with annealing temperature (Fig. 8). Further t → m transformation occurs at temperatures of 800–1100 °C and could be promoted by a remarkable increase of zirconia particle size.

Annealing of YSZ powders with yttria contents <3.9 mol % increases the fraction of monoclinic phase; however, the phase transformation starts at a temperature of about 1050 °C (Fig. 7). For the sample Z2.4Y, approximately 40% of the tetragonal phase transforms to monoclinic ZrO_2, but for the sample Z3.4Y, only about 15% of the tetragonal phase is unstable. Similarly, the fraction of monoclinic phase for pressed YSZ is higher than that of as-prepared powders with the value decreasing with increasing yttria content (Fig. 6). For pressed samples Z2.4Y and Z3.4Y about 80% and 20% of the tetragonal phase changes to monoclinic, respectively. No changes in the amount of tetragonal and cubic phases can be detected after annealing up to 1250 °C or pressing for YSZ samples with yttria contents higher than 3.9 mol %.

As was already mentioned above, plasma synthesis is characterized by a very short dwell time of reagents in the reaction zone. Particles formed at high temperature (~2000 K) are rapidly cooled down. Introduction of the quenching gas into the reaction chamber creates conditions when the quenching rate reaches a value of 10^4 K s^{-1}. For non-doped zirconia, the high-temperature tetragonal phase can be retained at room temperature. The content of the tetragonal phase increases with increasing specific surface area of the as-prepared powders, as it does with increasing quenching rate. This phase undergoes the transition to monoclinic zirconia under pressure or during annealing.

The absence of the stress-induced transformation and tetragonal-to-monoclinic transition during annealing at temperatures <1250 °C indicate that the tetragonal zirconia is the non-transformable t'-phase in as-prepared YSZ powders with an yttria content larger than 3.9 mol %. This phase forms by a diffusionless cubic → t' transformation if the material is rapidly quenched form the c-phase field through the (c + t) phases field [11]. Opposite the t-phase, it does not undergo stress-induced tetragonal-to-monoclinic transformation. The occurrence of the t → m transformation in powders with smaller than 3.9 mol % yttria is most likely caused by the inhomogeneity of yttria distribution among YSZ particles.

4. Conclusion

A plasma synthesis method has been developed to produce nanosized non-doped zirconia and YSZ powders with various yttria contents. The powders are synthesized by introducing a mixture of coarse-grained zirconia and yttria into an r.f. inductively coupled plasma flame. The average particle size of the as-prepared powders is in the range 20–40 nm and the specific surface area is 18–50 $m^2 g^{-1}$.

The phase and granulometric composition of the produced powders depend on the degree of evaporation of raw powders, reagent concentration in the gas flow and quenching rate, and on the content of Y_2O_3. Up to 5.5 mol % yttria, the major phase of nanosized powders is tetragonal ZrO_2, mostly as the non-transformable (t') form. For yttria contents higher than 6 mol %, the major phase is cubic ZrO_2.

Acknowledgement

This work was supported by Commission of the European Communities under project no. JOU2-CT92-0063, PL-2090.

References

1. D. L. BOURELL and W. KAYSSER, *J. Am. Ceram. Soc.* **76** (1993) 705.
2. M. SUZUKI, M. KAGAWA, Y. SYONO and T. HIRAI, *J. Mater. Sci.* **27** (1992) 679.
3. H. Y. LEE, W. RIEHENMANN and D. L. MORDIEKE, *Z. Metallkde* **84** (2) (1993) 79.
4. C. M. FOSTER, G. R. BAI, J. C. PARKER and M. N. ALI, *Mater. Res. Soc. Symp. Proc.* **286** (1993) 61.
5. G. P. DRANSFIELD, K. A. FOTHERGILL and T. A. EGERTON, *Euroceramics* **1** (1989) 275.

6. S. BHATTACHARJEE, U. SYAMAPRASAD, R. K. GALGALI and B. C. MOHANTY, *Mater. Lett.* **15** (1992) 281.
7. H. TORAYA, M. YOSHIMURA and S. SOMIYA, *J. Am. Ceram. Soc.* **67** (1984) c119.
8. N. IWAMOTO, N. UMESAKI and S. ENDO, *Trans. JWRI* **14** (1985) 89.
9. R. C. GARVIE, *J. Phys. Chem.* **82** (1978) 218.
10. M. KAGAWA, F. HONDA, H. ONODERA and T. NAGAE, *Mater. Res. Bull.* **81** (1983) 1081.
11. S. P. S. BADWAL, *Solid State Ionics* **52** (1992) 22.

Received 9 August 1996
and accepted 22 August 1997